Journal of Molecular Structure 1200 (2020) 127053

Contents lists available at ScienceDirect

Journal of Molecular Structure

journal homepage: http://www.elsevier.com/locate/molstruc

Single step synthesis of novel hybrid fluorescence probe for selective recognition of Pr(III) and As(III) from soil samples

Pinkesh G. Sutariya [a, *], Heni Soni [a], Sahaj A. Gandhi [b]

[a] Department of Chemistry, Bhavan's Shree I.L.Pandya, Arts-Science and Smt. J.M.Shah Commerce College, Sardar Patel University, V. V. Nagar, 388120, Gujarat, India

[b] Department of Physics, Bhavan's Shree I.L.Pandya, Arts-Science and Smt. J.M.Shah Commerce College, Sardar Patel University, V. V. Nagar, 388120, Gujarat, India

ARTICLE INFO

Article history:
Received 13 May 2019
Received in revised form
26 August 2019
Accepted 8 September 2019
Available online 12 September 2019

Keywords:
calix[4]arene
CHEF-PET
Computational study

ABSTRACT

Herein, the synthesis and evaluation of a novel CHEF-PET fluorescence sensor L, based on calix[4]arene comprising two 1-Naphthoicacid groups as binding sites, is described. The selective nature of this fluorescence probe towards Pr^{3+} and As^{3+} has been investigated by emission titration, UV–vis titration, ^1H NMR spectroscopy, FT-IR, PXRD and ESI-MS investigation. The linear concentration range at pH 3.5 of L for Pr^{3+} and As^{3+} is 0–120 nM and 0–145 nM respectively with the detection limit of 1.45 nM for Pr^{3+} and 1.91 nM for As^{3+}. Through Benesi-Hildebrand equation, the binding ability was found to be $7.377 \times 10^8\ M^{-1}$ for Pr^{3+} and $7.842 \times 10^8\ M^{-1}$ for As^{3+}. The MOPAC-2016 software package has been used to optimize the L using PM7 and the molecular docking study has been carried out using HEX software.

1. Introduction

The family of macrocycles has drawn much attention of many researchers in past few years for developing different effective molecular sensors. In the 70s, calixarene [1], a new family member of macrocycles was isolated and characterized by Gutsche [2] et al. apart from other members such as cyclodextrins, cucurbiturils, cryptands and crownethers. Though calixarenes have variety of derivatives like calix [4]arene, calix [6]arene and calix [8]arene; calix [4]arene has been counted as the most relevant framework for constructing ion-selective sensors. By functionalizing calix [4]arene at its upper and lower rim, the power of encapsulating many different ions is increased and it works as very effective host molecule [3–11].

Metals such as Fe^{2+}, Cu^{2+}, Mn^{2+} and Zn^{2+} are present in human body while Pr^{3+}, La^{3+} and Nd^{3+} exist in different soil samples whereas water contains As^{3+} and Hg^{2+} as impurities. In short, metals subsist in different forms with different quantities everywhere. This has been inspiring for researchers to develop such molecular sensors which can detect metal ions easily with its well-defined binding core. Fluorescence signalling is one the most appropriate techniques to recognize metal ions through tangible fluorescence signals. The combination of calix [4]arene and fluorescence signalling technique results into edifice simple, selective and affordable fluorescence probe.

In photoinduced electron transfer (PET), the energy of the HOMO of the free host lies between those of the HOMO and LUMO of the excited fluorophore and then electron transfer from the HOMO of the Host to the hole in the HOMO of the fluorophore takes place. PET process always follow quenching of emission intensity when guest molecular ions bind to host. Photoinduced charge transfer (PCT) mechanism has been involved in those fluoroionophore which contain electron withdrawing and electron-donating substituents, this charge transfer may arise over long distances and be connected with major dipole moment changes, making the process particularly sensitive to the microenvironment of the fluoroionophore. Another class of fluoroionophores, where intramolecular interaction between a pair of different fluorophores in which one acts as a donor of excited-state energy to the other (acceptor). As a result that the donor returns to its electronic ground state and emission may then occur from the acceptor center. This process is known as fluorescence resonance energy transfer (FRET). There are also few other mechanism in calix [4] arene system such as metal-ligand charge transfer (MLCT), proton transfer, formation of an excimer and chelation-enhanced fluorescence (CHEF) for the molecular recognition [12–22].

* Corresponding author.
E-mail address: pinkeshsutariya@gmail.com (P.G. Sutariya).

https://doi.org/10.1016/j.molstruc.2019.127053
0022-2860/

Among all lanthanoides, Praseodymium (III) ion is one of the rare chemical which can be found in house equipment such as television, fluorescent lamps, energy saving lamps and glass. It is also used in carbon arc lights in the motion picture industry. It is predominantly used as an alloying agent with magnesium to create high-strength metals which are used in aircraft engines. Pr^{3+} is very dangerous in working atmosphere and can cause damage to reproduction and nervous system of animals [23,24]. Arsenic is a naturally occurring element that is widely spread in the Earth's crust. It is found in water, air, food, and soil. Scientists, paediatricians and public health advocates are progressively anxious about the more subtle and long-range health effects of low-level exposures to humans, especially for infants and children exposed to arsenic in water and some foods, such as rice-based products, during sensitive windows of development. Most arsenic gets into the body through absorption of food or water. Arsenic in drinking water is a problem in many countries around the world, including Bangladesh, Chile, China, Vietnam, Taiwan, India, and the United States. Arsenic affects a broad range of organs and systems including: skin, nervous system, respiratory system, cardiovascular system, liver, kidney, bladder and prostate [25–27]. Therefore, it is necessary to develop receptors which can selectively sense such ions of vital trace elements and biologically important cations by spectroscopy.

The requisite of various molecular sensors has driven us to synthesize different fluorescence receptors for selective recognition and determination of Zn^{2+}, Cu^{2+}, Cd^{2+}, Sr^{2+}, Fe^{3+}, F^{-}, phosphate ions, L-Tryptophan and L-Histidine [28–34]. Though some reports are available for the selective recognition of Pr^{3+} and As^{3+} by calix [4]arene conjugates, to our knowledge, there is no report in the literature wherein a single system can sense both ions. Further, the structural characterization of the species of recognition is rather scarce in the literature. The probe would be useless if it would not be used in real samples of Pr^{3+} and As^{3+}. By keeping that in mind, we have also carried out experiments of our fluorescence probe in soil samples. The demand of multi-ion selective fluorescence probe has motivated us to make a convenient, fast responsive, highly selective and sensitive fluorescence sensor; so here we are proposing a simple, sensitive and selective system, with fast response time and low detection limit calix [4]arene linked fluorescence probe Synthetic route for 5, 11, 17, 23-tetra t-butyl-26, 28 dimethoxy 25, 27 dicarboxylate naphthalene calix [4]arene (L) receptor (Fig. 1, Scheme 1) which displays CHEF-PET phenomenon in selective recognition of Pr^{3+} and As^{3+}.

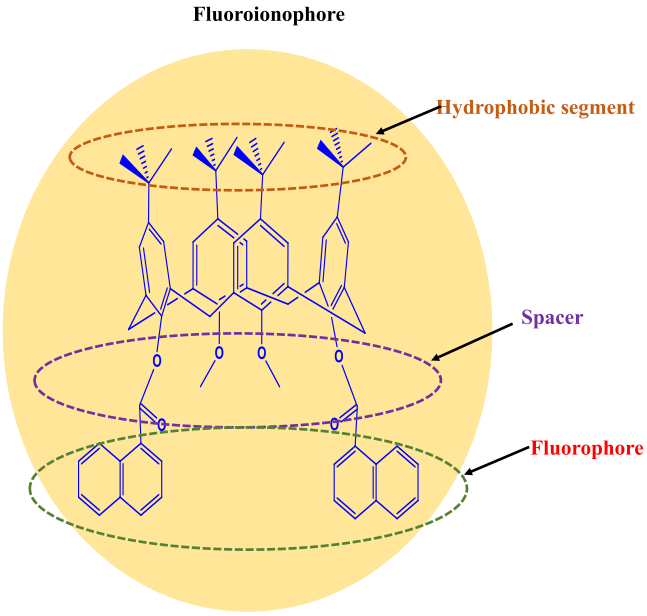

Fig. 1. Schematic design of synthesized scaffold L.

2. Experimental

2.1. Chemicals and reagents

All the reagents and chemicals like DCC (N, N′-dicyclohexylcarbodiimide), DMAP (4-dimethylaminopyridine) and 1-Naphthoicacid were used of analytical grade procured from Sigma Aldrich. Silica gel (Merck, 0.040–0.063 mm) was used for column chromatography. Metal salts (99–101% purity of SRL) used for the studies were their perchlorate salts (Caution: Since perchlorate salts are known to explode under certain conditions, these are to be handled cautiously!) with formula, $M(ClO_4)_2.xH_2O$. Anions used for the studies were their tetra butyl ammonium salts (99–101% purity of SRL) which were prepared in acetonitrile. Stock solutions of cations and anions (0.01 M) are prepared in acetonitrile. Further dilutions are completed as per requirement. Spectroscopic properties of L was investigated in mixed aqueous organic medium [citric acid buffer; pH = 3.5)].

2.2. Apparatus

Melting points were taken on Opti-Melt (Automated melting point system). FT-IR spectra were recorded as KBr pellet on Bruker TENSOR-27 in the range of 4000–500 cm^{-1}. Discover Bench Mate system-240 V (CEM Corporation) microwave synthesizer was used for synthesis of p-tertbutylcalix [4]arene. GmbH Vario Micro cube elemental analyzer was used for elemental analysis. ^1H NMR spectra was scanned on 400 MHz FT-NMR Bruker Avance-400 in the range of 0.5–15 ppm using internal standard tetramethylsilane (TMS) and deuterated DMSO as a solvent. ESI Mass spectra were taken on a Shimadzu GCMS-QP 2000A. Emission spectrum was recorded on Horiba Jobin, Fluorolog, and Edinburgh F900. UV–Vis absorption spectra were acquired on a Jasco V-570 UV–Vis. Spectrometer. Working standard solutions were prepared daily in deionized water. The crystalline phase of the synthesized samples were identified by powder X-ray diffractometer (PXRD), non-destructive fingerprinting technique (PANalytical X-ray diffractometer), recorded with Cu Kα radiation (λ = 1.54060 Å) operating at 40 kV and 30 mA.

2.3. Real sample preparation

For the analytical application of proposed fluorescence probe, we have applied this probe for real sample analysis in soil sample for Pr^{3+} and As^{3+}. For soil sample preparation, we collected soil samples from industrial area of Anand GIDC, Gujarat, India for analysis. The soil samples were first dissolved in concentrate HNO_3 and stirred for 1 h after then we took 10 mL of solution and diluted up to 100 mL into volumetric flask. From this solution, we took 2 mL of solution and 2 mL of our synthesized ligand L for fluorometric analysis by maintaining pH 3.5 with citric acid buffer. This experiment carried out by using in situ generated Pr^{3+} and As^{3+} complex of L with various soil samples. The concentration range during this experiment was 0–100 nM. This result authorizes the application of L as fluroionophore having high sensitivity and specificity towards Pr^{3+} and As^{3+} detection in soil samples.

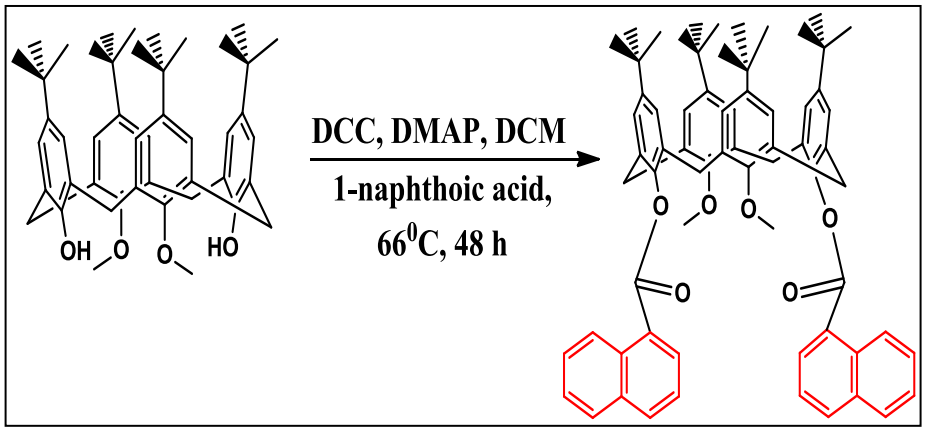

Scheme 1. Synthetic route for 5, 11, 17, 23-tetra t-butyl-26, 28 dimethoxy 25, 27 dicarboxylate naphthalene calix [4]arene (L) receptor.

2.4. Experimental

2.4.1. Synthesis of 5, 11, 17, 23-tetra t-butyl-25, 27 dimethoxy calix [4]arene

A mixture of p-tert-butyl calix [4]arene A (3.5 g. 0.80 mM), K_2CO_3(1.9 g, 14.0 mM) and 1-iodomethane (4 mL, 14.0 mM) in dry acetone (150 mL) was stirred for 24 h. The actual reaction time was considered by taking thin layer chromatography (tlc) at regular interval of time by using mixture of ethylacetate:hexane (8:2). The solvent was then evaporated under vacuum and the residue taken up with CH_2Cl_2. The organic phase was washed with 0.1 M HCl up to neutrality and dried over anhydrous Na_2SO_4. After complete evaporation of the solvent, the resulting crude product was purified by column chromatography (silica gel, hexane: ethyl acetate, 9:1); **Solubility**: Soluble in $CHCl_3$, CH_2Cl_2, CH_3CN and insoluble in H_2O, **Yield** 2.9 g (81%). **Elemental analysis for $C_{46}H_{60}O_4$**: C, 81.61; H, 8.93% **Found**: C, 81.38; H, 8.52%. **FT-IR (KBr)** υ: 3280 cm^{-1}(Ar-CH), 3430 cm^{-1}(Ar-OH). **^{1}H NMR**: δ_H ($CDCl_3$,500 MHZ), 1.20 (18H, tbutyl, s) 0.96(18H, *t*-butyl, s), 4.28 (4H, $-OCH_3$, t), 3.83 (4H, $ArCH_2Ar$,d), 4.30(4H, $ArCH_2Ar$, d), 6.42(4H, Ar−H, s), 6.85(4H, Ar−H, s), 9.19 (2H, OH, s), **m. p.** 223-228^{O}C. **ESI MS (m/z)** 677.1 (M+1).

2.4.2. Synthesis of 5, 11, 17, 23-tetra t-butyl-26, 28 dimethoxy 25, 27 dicarboxylate naphthalene calix [4]arene (L)

A solution of compound 5, 11, 17, 23-tetra t-butyl-25, 27 dimethoxy calix [4]arene (0.5 g), DCC (0.25 g), DMAP (0.15 g) and 1-naphthoicacid (0.27 g) in DCM solvent was stirred for 48 h. The actual reaction time was considered by taking thin layer chromatography (tlc) at regular interval of time by using mixture of chloroform: methanol (3.5: 1.5). The solvent was then evaporated under vacuum. Yield: 0.820 g, (90%). Anal calcd for $C_{68}H_{72}O_6$: calcd C, 82.89; H, 7.37; O, 9.74. Found: C, 82.61; H, 7.18. FT-IR: 1678 cm^{-1} (-C═O), ^{1}H NMR (400 MHz, DMSO): δ 7.51 (dd, 8H, Ar−H), 7.60 (dd, 4H, Ar−*H*), 7.61 (dd, 8H, Ar−H), 7.90 (dd, 4H, Ar−H), 7.92 (dd, 2H, Ar−H), 8.04 (dd, 2H, Ar−H), 8.22 (dd, 2H, Ar−H), 8.91 (dd, 2H, Ar−H), 8.92 (dd, 2H, Ar−H), 4.70 (d, 8H, $ArCH_2Ar$), 3.48 (s, 6H, $-CH_3$), 1.89 (s, 18H, $-C(CH_3)_3$), 1.38 (s, 18H, $-C(CH_3)_3$), ESI MS (*m/z*): found 986 (m+1).

2.5. Photo physical behaviour

Absorption spectra of the newly synthesized lower rim substituted calix [4]arene dimethoxynaphthoicacid **(L)** was recorded in all the solvents in which it is soluble, however acetonitrile was selected for further studies since acetonitrile is miscible with water. This compound shows absorption peak in the region between 250 and 380 nm, the peak at 284 nm indicates π- π* transition of 1-Naphthoicacid system. This compound shows a strong luminescence peak at 371 nm in acetonitrile with excitation at the absorption maxima (λ_{max}) of the 1-Naphthoicacid moiety, which is at 200−450 nm.

2.6. General screening of fluorescence probe L with various ions

Since our fluorescence probe L possesses binding cores (Scheme- 1), the ion-selective properties of L with various cations (Zn^{2+}, Cd^{2+}, Fe^{2+}, Fe^{3+}, La^{3+}, As^{3+}, Nd^{3+}, Zr^{4+}, Ca^{2+}, Ce^{3+}, Li^{+}, Ag^{+}, Ba^{2+},Co^{2+}, Hg^{2+}, Na^{+}, K^{+}, Cu^{2+}, Ni^{2+}, Mn^{2+}, Cr^{3+}, Pb^{2+} and Sr^{2+}) have been studied by the fluorescence spectroscopy, absorption spectroscopy, FT-IR and ESI-MS investigation. The binding affinity of L with cations was investigated by making stock solutions of the compound L (1×10^{-8} M) and that of perchlorate salts (1×10^{-6} M) of aforesaid metal ions prepared in freshly purified acetonitrile as acetonitrile is miscible with water. Then 2.5 mL stock solution of the compound and 2.5 mL stock solution of each metal salts were taken in a 5 mL volumetric flask, so that the effective concentration of the metal is 100 fold than that of the compound L. Further to determine the connection of the metal ions with the ionophore, the spectra of the cations added solutions were compared with that of the original solution. Spectroscopic properties of L was investigated in mixed aqueous organic medium [citric acid buffer; pH = 3.5)].

3. Results and discussion

3.1. Emission titration of L

To examine the spectroscopic properties of ligand L, we have used mixed aqueous organic medium [citric acid buffer; pH = 3.5)]. Naphthalene has been extensively used as fluorophore for the detection of molecular ions [35]. Herein, we are proposing a calix [4]arene-based fluoroionophore armed by two naphthoic acid groups as binding sites. We have noted an on/off/on fluorescent effect by using our new ligand L having naphthoic acid as two armed binding sites. In this ligand L, due to the absence of nitrogen atom, anions cannot bind with ligand L and do not show any changes in the fluorescence intensity. That's why, here we have intentionally neglected anions. In the absence of Pr^{3+}, the fluorescence is partially quenched because of photoinduced electron transfer (PET) effect. However, studies indicate that this CHEF effect was perceived due to the inhibition of PET mechanism. The fluorescence spectra of the compound was recorded in acetonitrile in presence of 100-fold excess of various cations and anions which

were prepared in acetonitrile. We evaluated the interaction of ligand with Pr^{3+} and As^{3+} in the presence of other cations and anions. The sensing ability of our fluoroionophore was explored by adding 1×10^{-6} M solutions of Pr^{3+} and As^{3+} into 1×10^{-8} M solution to the fluoroionophore (L). From the fluorescence spectra, we observed that the intensity of L was enhanced because of CHEF effect between L and Pr^{3+} whereas As^{3+} quenched the fluorescence intensity of L via PET.

3.2. Selectivity of Pr^{3+} and As^{3+} with L based CHEF-PET probe

To obtain insight into the selective nature of our newly synthesized probe L, we have carried out ion-binding study by using various perchlorate salts of metal ions (Zn^{2+}, Cd^{2+}, Fe^{2+}, Fe^{3+}, La^{3+}, As^{3+}, Nd^{3+}, Zr^{4+}, Ca^{2+}, Ce^{3+}, Li^{+}, Ag^{+}, Ba^{2+}, Co^{2+}, Hg^{2+}, Na^{+}, K^{+}, Cu^{2+}, Ni^{2+}, Mn^{2+}, Cr^{3+}, Pb^{2+} and Sr^{2+}) with ligand L. In this experiment, we have kept equal concentration (1×10^{-8} M) for L and numerous above mentioned perchlorate salts in acetonitrile. From the emission spectra, depicted in Fig. 2, we observed clear changes upon addition of Pr^{3+} and As^{3+} when it is compared to the spectra of original ligand L. By contrast, no significant changes were noticed upon addition of other cations into ligand L. Pr^{3+} and As^{3+} induced enhancement and quenching in the fluorescence intensity of the ligand L by displaying ON-OFF-ON behaviour. The overall emission changes were dramatic: 2.25 fold for Pr^{3+} and 0.001 fold As^{3+} with L (Fig. 2 A). Therefore it is predicted that Pr^{3+} and As^{3+} closely interact with L and cause obvious change in fluorescence intensities with respect to other large number of cations and anions. Hence, for quantitative analysis we have selected these two ions (Pr^{3+} and As^{3+}) for further examination.

3.3. Sensitivity of L based CHEF-PET probe

As sensitivity is a vital part for any chemosensor, fluorescence titration has pursued by gradually varying the concentration of Pr^{3+} (0–120 nM) and As^{3+} (0–145 nM) by keeping the concentration of L constant [Fig. 2 (B–C)]. For the mechanism of emission quenching, stern–volmer plots are worthwhile and that is why they are used to analyze the nature of the quenching process in the chelating complex L-As^{3+}. As shown in equation (1), the determination of dynamic or static quenching process can be examined by plotting relative emission intensities (I_0/I) against quencher concentration [Q] in which the slope of the plotted line yields K_{sv} (the static quenching constant).

$$\frac{I_o}{I} = 1 + Ksv[Q] \quad (1)$$

where Io/I and [Q] are the relative emission intensity and quencher concentration, respectively.

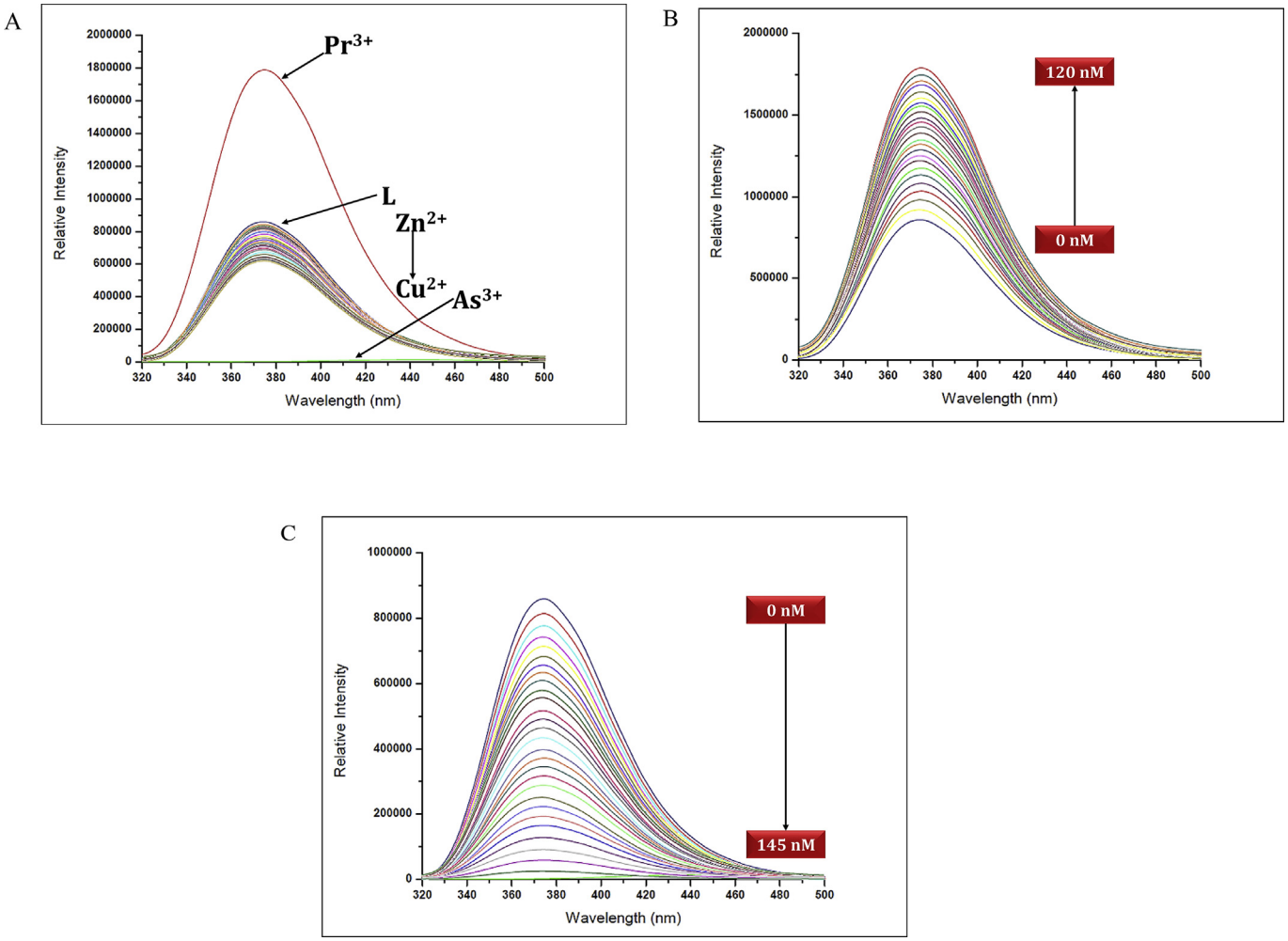

Fig. 2. (A): Selectivity plot of L (1×10^{-8} M) with various cations from top to bottom (Zn^{2+}, La^{3+}, Co^{2+}, Cd^{2+}, Mn^{2+}, Fe^{3+}, Hg^{2+}, Nd^{3+}, Zr^{4+}, Ca^{2+}, Ce^{3+}, Li^{+}, Ag^{+}, Ba^{2+}, Na^{+}, K^{+}, Ni^{2+}, Pb^{2+}, Sr^{2+}, Fe^{2+} and Cu^{2+}).

In our case, typical linear plots for L-As^{3+} suggest a pure fluorescence static quenching because of a non-fluorescence ground state complex between ligand L and As^{3+}. The calibration curve shows good linearity with correlation coefficient of 0.9944 for Pr^{3+} and 0.9901 for As^{3+} [Fig. 3 (A–B)]. We have also calculated limit of detection (LOD) as per 3σ IUPAC criteria for synthesized probe from this emission study. The LOD was found to be 1.45 nM for Pr^{3+} and 1.91 nM for As^{3+}.

3.4. Binding constant of L based CHEF-PET probe for Pr^{3+} and As^{3+}

Binding constants for fluoroionophore were calculated by using emission titration data following the previously reported articles [36,37]. Here, we have displayed representative spectra showing the changes observed in emission intensities upon the addition of increasing concentration of ions. According to this method, the fluorescence intensity (F) scales with the metal ion concentration ([M]) through $(F_0–F)/(F\text{-}F_\infty) = ([M]/K_{diss})^n$. The binding constant ($K_s$) is obtained by plotting

$$\boldsymbol{Log}\,\frac{(\mathbf{F}_0-\mathbf{F})}{(\mathbf{F}-\mathbf{F}_\infty)}=\boldsymbol{Log}\,[\boldsymbol{M}]$$

where F_0 and F_∞ are the relative fluorescence intensities without addition of guest metal ions and with maximum concentration of metal ions (when no further change in emission intensity takes place), respectively. The value of Log [M] at $Log[(F_0–F)/(F\text{-}F_\infty)] = 0$ gives the value of $log(K_{diss})$, the reciprocal of which is the binding constant (K_s). The observed binding constant from fluorescence spectra for Pr^{3+} and As^{3+} are respectively $7.377 \times 10^8\ M^{-1}$ and $7.842 \times 10^8\ M^{-1}$ (Fig. 4A and B).

3.5. Quantum yield of L with Pr^{3+} and As^{3+}

The quantum yield was calculated by following equation (2)

$$\phi = \phi\text{std}\,\frac{(F \times Astd \times \eta)}{(Fstd \times A \times \eta std)}$$

where F and F_{std} are the areas under the fluorescence emission curves of the Pr^{3+} and As^{3+} ions complexes with L and only standard L respectively. A and A_{std} are the areas under relative absorbance of the Pr^{3+} and As^{3+} ions complexes with L and standard L at the excitation wavelength, respectively. η and η_{std} are the refractive indices of solvent (acetonitrile) used for the Pr^{3+}, As^{3+} and standard (L), respectively. The Pr^{3+}, As^{3+} and the standard (L) were excited at the same wavelength. The quantum yield of fluoroionophore L was obtained using emission spectra of standard fluorophore (naphthalene). The reported quantum yield of naphthalene [38] was approximately 0.23 and that of L with Pr^{3+} and As^{3+} ion complex were found to be 0.47 and 0.0003 respectively. Thus, when Pr^{3+} was attached to L, the quantum yield increases whereas for As^{3+}; quantum yield decreases. Hence L provides a sensitive means to recognize Pr^{3+} and As^{3+} by direct fluorescence measurement.

3.6. UV–visible experiment

In addition to confirm the binding event of probe L, UV–visible investigation was performed in acetonitrile medium. The free ligand L displayed a strong absorption band at 284 nm. When Pr^{3+} and As^{3+} (as their perchlorate salts in acetonitrile) were added to the solution of L, the change in absorption band was observed. The selective nature of probe L towards Pr^{3+} and As^{3+} was confirmed by noticing the change in absorption band from 284 nm to 268 nm and 278 nm upon addition of Pr^{3+} and As^{3+} respectively (Fig. 5A–B). The change in shift indicates bathochromic shift because of cation binding with ketonic group of the scaffold. To know the detection limit of L towards Pr^{3+} and As^{3+}, we have also performed UV–vis titration by varying concentration of selective ions (0 nM–100 nM) (Fig. 5C–D). From this investigation, we can assure that when it is matter of sensitivity and low detection limit, fluorescence technique is more reliable than absorption study.

3.7. ESI-MS investigation

For further binding confirmation of Pr^{3+} and As^{3+} with ligand L, we have implemented ESI-MS technique. The complex was dissolved in CH_3CN (3 mL) and 10 equivalent amount of the desired cations as perchlorate salt were added into the solutions. The reaction mixtures were stirred at room temperature for 2 h, the solutions were then filtered off and the filtrates were analysed by ESI MS instrument. The formation of 1:1 complex was confirmed by ESI-MS, where the spectrum shows molecular ion peak *m/z* at 984.53 whereas in the presence of Pr^{3+} and As^{3+} show peak at 1125.44, 1059.45 respectively (Fig. 6A–B). These results will give assurance of binding of Pr^{3+} and As^{3+} with L ligand via electrostatic interaction.

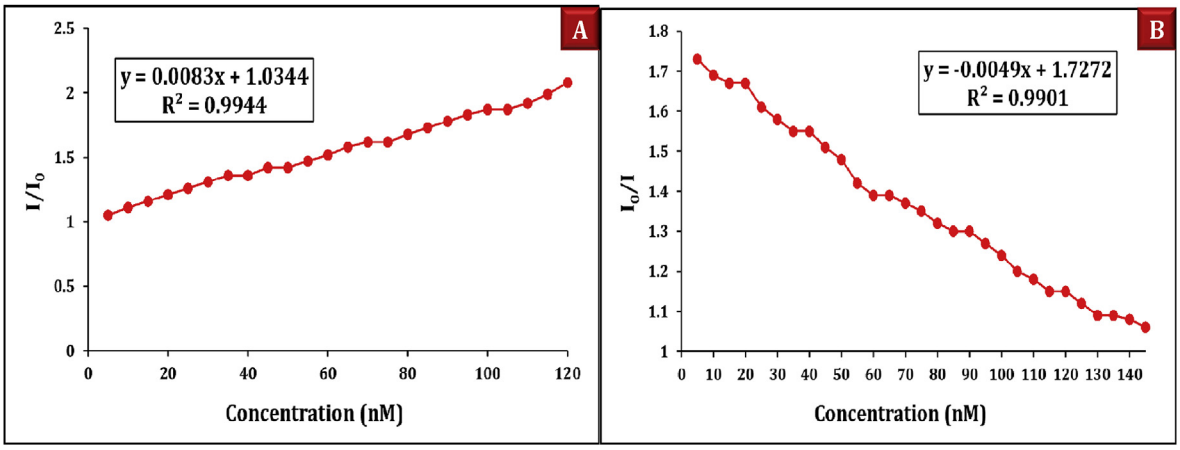

Fig. 3. (A–B): (A) Linearity plots of L (1×10^{-8} M) with Pr^{3+} (0–120 nM) and (B) As^{3+} (0–145 nM).

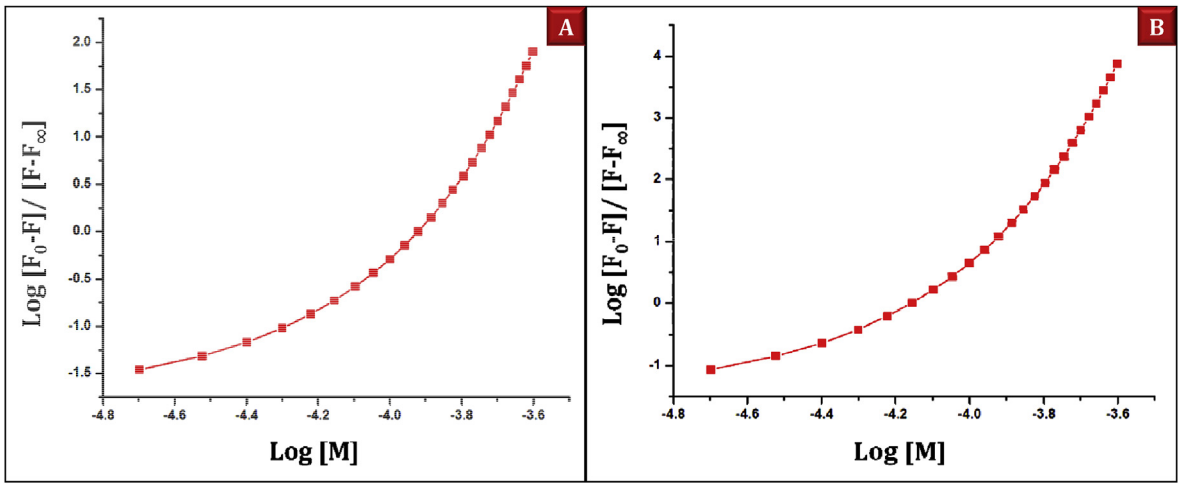

Fig. 4. (A–B): Binding constant plots for (A) Pr^{3+} and (B) As^{3+} with L ligand from emission titration.

3.8. FT-IR comparative analysis

The FT-IR spectra of pure ligand L, L + Pr^{3+} and L + As^{3+} were recorded by potassium bromide (KBr) disk method and scanned at the wave number region 4000-500 cm^{-1}. Moreover, FT-IR comparative experiment was also executed in which the binding of Pr^{3+} and As^{3+} with ligand L was evaluated. The broadening of −CH aromatic stretching peak and change in −C═O(ketone) peak in presence of Pr^{3+} and As^{3+} will give assurance of effective binding of Pr^{3+} and As^{3+} with L. [Fig. S2 (ESI†)].

3.9. Effect of pH on L CHEF-PET probe and binding mechanism

For making a chemosensor work effectively, it is also necessary

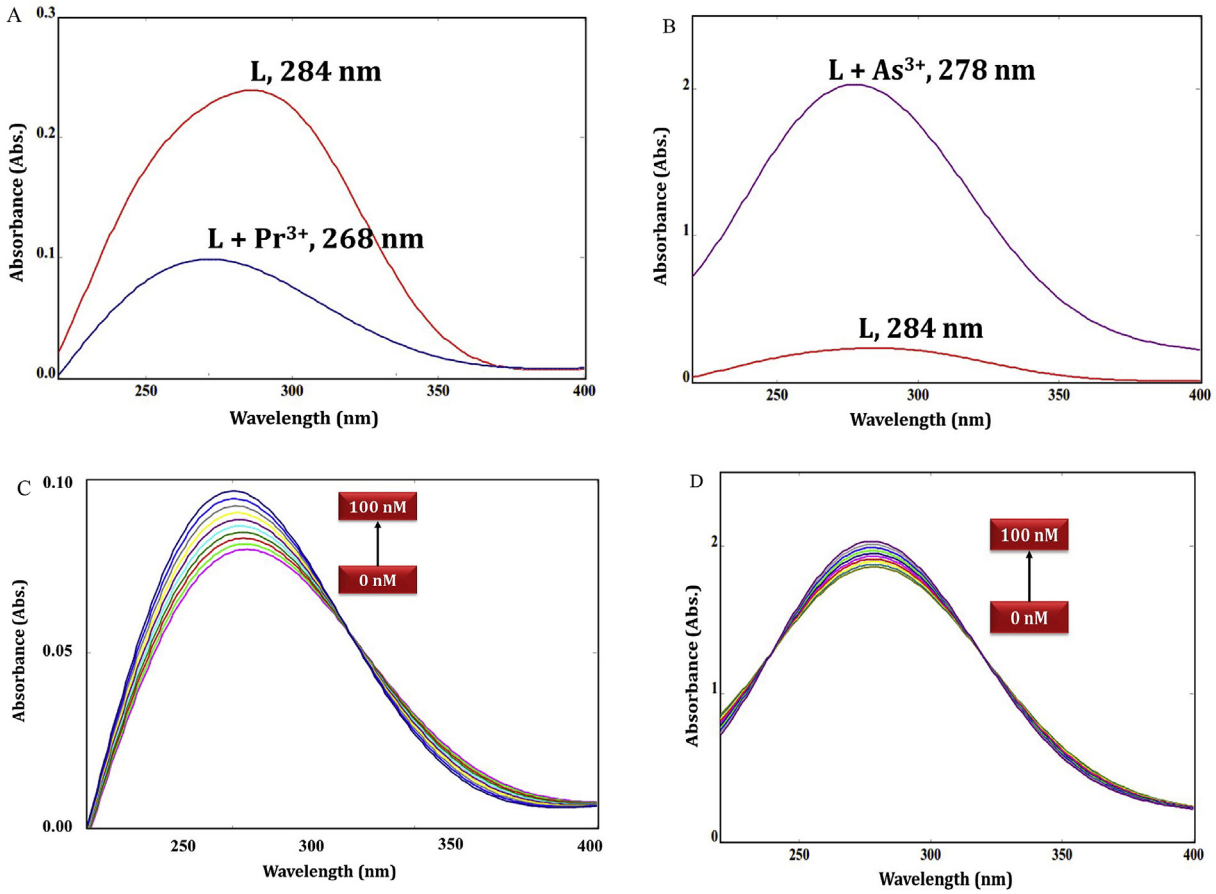

Fig. 5. (A): Absorption spectral changes of L (1×10^{-6} M) ligand in the presence of Pr^{3+}.(B): Absorption spectral changes of L (1×10^{-6} M) ligand in the presence of As^{3+}.(C): The plot demonstrates the absorption spectral changes of L (1×10^{-6} M) in the presence of different concentrations of Pr^{3+}. (0, 10 nM, .100 nM).(D): The plot demonstrates the absorption spectral changes of L (1×10^{-6} M) in the presence of different concentrations of As^{3+}. (0, 10 nM, .100 nM).

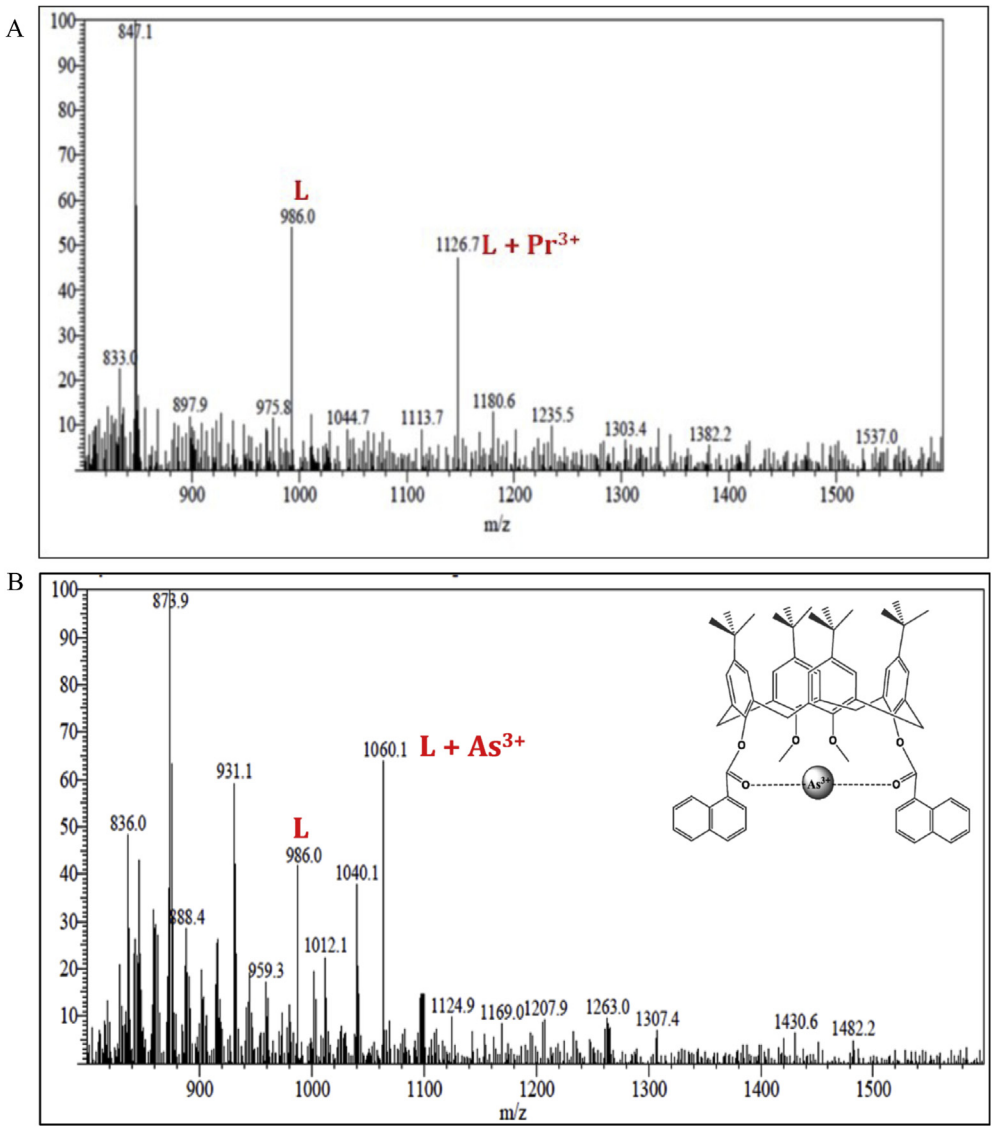

Fig. 6. (A): ESI mass spectrum showing the isotopic peak pattern of molecular ion peak for 1:1 complex formed between L and Pr^{3+}.(B): ESI mass spectrum showing the isotopic peak pattern of molecular ion peak for 1:1 complex formed between L and As^{3+}.

to check the nature of ligand L in various pH conditions. As shown in [Figs. S3–S4 (ESI†)], the fluorescent ligand L displays maximum enhancement for Pr^{3+} and quenching for As^{3+} at pH 3.5. This is due to C═O linkage which makes it acidic in nature. From this investigation, we can say that our chemosensor will act effectively in acidic condition. By performing UV–visible experiment, the stoichiometry of the complex formed (1: 1) has been also derived based on the Job's plot [Figs. S5–S6 (ESI†)]**.** The reason behind enhancement and quenching in fluorescence intensity of ligand L is that Pr^{3+} and As^{3+} interact with ketonic group of L ligand.

3.10. Interference study

From our ion-binding study, we have concluded that Pr^{3+} enhanced and As^{3+} quenched the fluorescence intensity of ligand L. However, it is important to check whether the chemosensor responds effectively towards Pr^{3+} and As^{3+} in the presence of other metal ions. In order to identify the real potential ability of our probe L, we have pursued an interference study. As depicted in Fig. 7**,** the fluorescence response of the chelated complex (L-Pr^{3+} and L-As^{3+}) with other competing ions showed an obvious fluorescence enhancement and quenching as aforesaid technique even in the presence of other cations and anions. From this competitive titration, we have determined that other cations are unreactive towards the chemosensor L except Pr^{3+} and As^{3+}. Proposed binding mechanism through hydrogen bonding and electro static interaction with L ligand by Pr^{3+} and As^{3+} is shown in Fig. S7 (ESI†).

3.11. Real sample analysis

This CHEF-PET probe is applied for its important applicability to sense Pr^{3+} in soil samples by using fluorescence titration and also confirmed the stability of metal-complex. The standard addition method was applied to evaluate the validity of the proposed sensor. Table 1 demonstrates analytical results of them. The result gained with excellent recovery of spiked Pr^{3+} ranged from 94 to 99%, proving the validity of the developed technique. Furthermore, this fluoroionophore has been applied for As^{3+} ion detection from soil samples and its results are shown in Table 2. The concentration of each sample was measured by the CHEF-PET sensor, using the

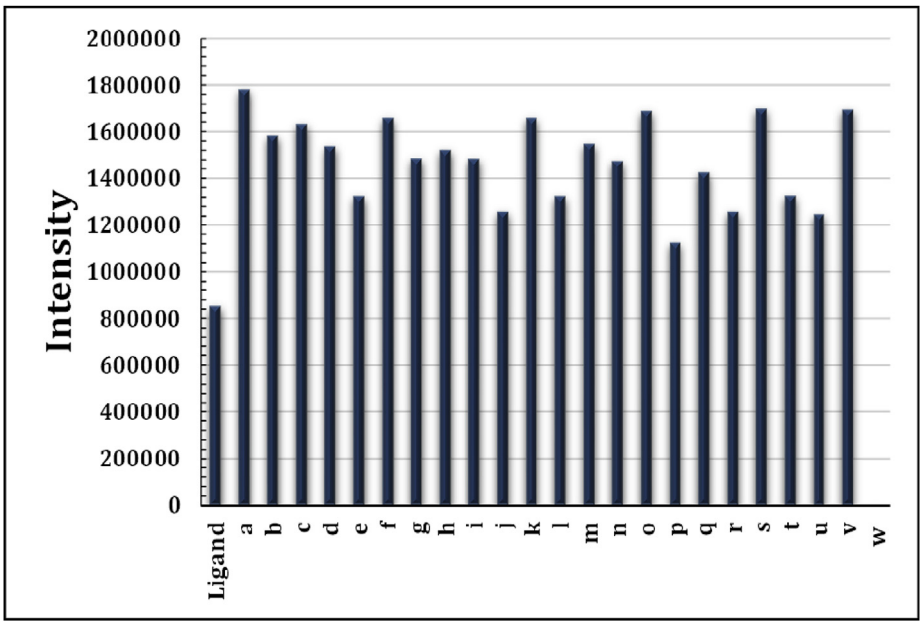

Fig. 7. Competitive emission spectra of L (1×10^{-8} M) with Pr^{3+} in presence of other cations (a = Ligand + Pr^{3+}, b = a + Zn^{2+}, c = a + La^{3+}, d = a + Co^{2+}, e = a+ Cd^{2+}, f = a+ Mn^{2+}, g = a+ Fe^{3+}, h = a + Hg^{2+}, i = a+ Nd^{3+}, j = a + Zr^{4+}, k = a + Ca^{2+}, l = a + Ce^{3+}, m = a + Li^{+}, n = a + Ag^{+},o = a + Ba^{2+}, p = a + Na^{+}, q = a + K^{+}, r = a + Ni^{2+},s = a + Pb^{2+},t = a +Sr^{2+}, u = a + Fe^{2+}, v = a + Cu^{2+} and w = a + As^{3+}).

Table 1
Results of the determination of Pr^{3+} in industrial water sample.

Sample	Spiked Pr^{3+} (nM)	Found by AAS (nM)	Found by proposed sensor (nM)	Recovery (%)
Industrial Water Sample 1	10	9.75	9.41	96.51 ± 0.5
Industrial Water Sample 2	20	19.34	19.10	98.75 ± 0.6
Industrial Water Sample 3	30	28.89	28.24	97.75 ± 0.3
Industrial Water Sample 4	40	39.46	39.18	99.2 ± 0.7
Industrial Water Sample 5	100	98.80	98.13	99.32 ± 0.3

†Electronic Supplementary Information (ESI) contains materials and methods, synthesis procedure, ^{1}H NMR spectra, FT-IR spectra graph, pH investigation spectra, Job's plot and computational work.

calibration method. The proposed technique is compared with reported methods for determination of Pr^{3+} and As^{3+} (Table 3). This comparison undoubtedly endorses that proposed fluorometric method is superior to others in terms of sensitivity, selectivity and binding ability to recognize Pr^{3+} and As^{3+} [27,39–43].

3.12. Powder X-ray diffraction experiment of L-Pr^{3+} and L-As^{3+}

The powder diffraction pattern of the ligand L ($C_{68}H_{72}O_6$), L + As^{3+} ($C_{68}H_{72}O_6As^{3+}$) and L + Pr^{3+} ($C_{68}H_{72}O_6Pr^{3+}$) are presented in Fig. 8. The experimental 2θ range 5.00–80.00° with a step size of 0.01° and a counting time of 60s per step. Fig. 8 displayed highly intense peaks at 2θ values 7.68° (012), 28.02° (−102) and 35.57° (121) of ligand L, metal complexes L + As^{3+} and L + Pr^{3+} respectively. From the overly of PXRD patterns of metal complexes, new peaks and shifting of peak was observed due to the presence of As^{3+} and Pr^{3+} with ligand L. The lattice parameters of the unit cell and determination of the space group were calculated using match program (phase identification from powder diffraction), tabulated in Table S1. It reveals that ligand L and As^{3+} complex belong to the triclinic system with $P\bar{1}$ space group and Pr^{3+} has monoclinic crystal system with space group $P2_1/c$. Analytical indexing of the

Table 2
Results of the determination of As^{3+} in industrial water sample.

Sample	Spiked As^{3+} (nM)	Found by AAS (nM)	Found by proposed sensor (nM)	Recovery (%)
Industrial waste water sample 1	10	9.82	9.26	94.29 ± 0.4
Industrial waste water sample 2	20	18.98	18.51	97.52 ± 0.2
Industrial waste water sample 3	30	29.62	29.27	98.81 ± 0.6
Industrial waste water sample 4	40	38.81	38.39	98.91 ± 0.5
Industrial waste water sample 5	100	98.87	98.43	99.55 ± 0.3

Table 3
Comparative table of previously reported method with our developed method.

Method	Recognized ion	Linear range	Limit of detection	Ref.
Ion Selective electrode	Pr^{3+}	1.0×10^{-3} to 1.0×10^{-8} M	7.0×10^{-9} M	27
Ion Selective electrode	Pr^{3+}	1.0×10^{-2} to 1.6×10^{-6} M	6.0×10^{-2}	39
PVC membrane sensor	Pr^{3+}	1.0×10^{-8} to 1.0×10^{-2} M	5.0×10^{-9} M	40
Colorimetric sensor	As^{3+}	5.0–100 ppb	7.2 ppb	41
Nanoporous gold microelectrode (Anodic stripping voltammetry)	As^{3+}	10–200 μg L^{-1} - 2–30 μg L^{-1}	0.62 μg L^{-1}	42
Electrochemical detection	As^{3+}	0.002–0.8 mM	20 nM	43
Present method	Pr^{3+} and As^{3+}	0–120 nM for Pr^{3+} and 0–145 nM for As^{3+}	1.45 nM for Pr^{3+} and 1.91 nM for As^{3+}	–

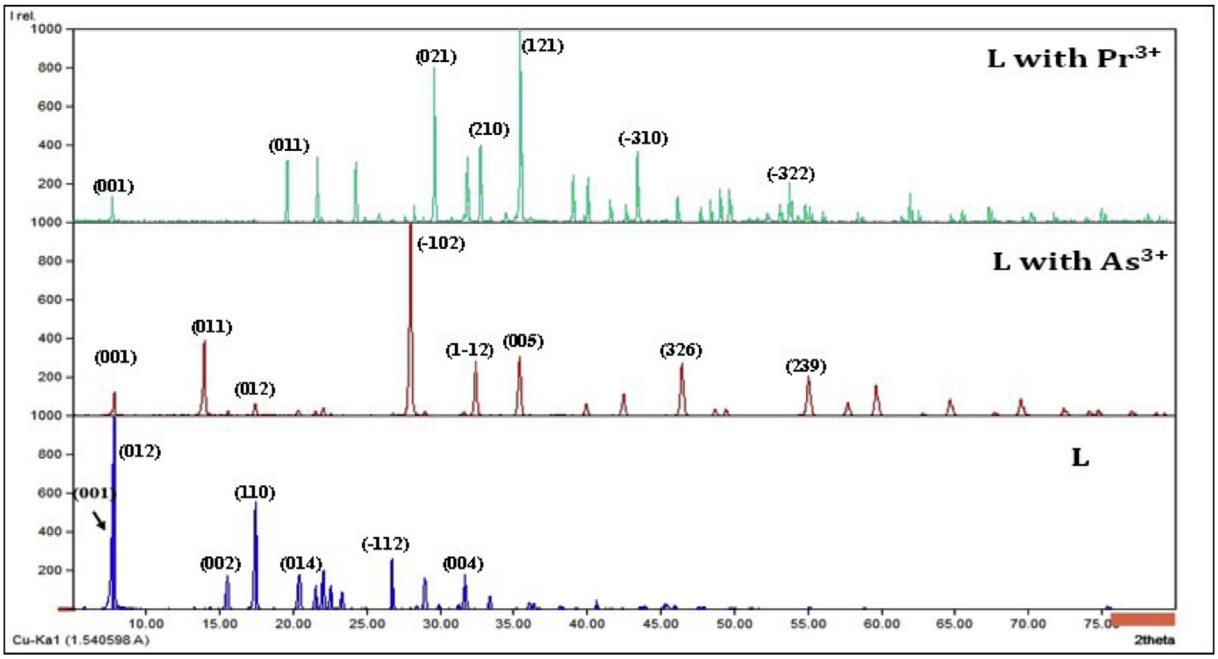

Fig. 8. Comparative PXRD investigation of the ligand L, L with As^{3+} and L with Pr^{3+}.

powder patterns for ligand L, L with As^{3+} and L with Pr^{3+} were summarized in Tables S2–S4 respectively. The PXRD investigation will give assurance of cationic (Pr^{3+} and As^{3+}) binding of with ligand L with 1:1 stoichiometry.

3.13. Computational investigation

The important intended of computational experiment is to optimize geometry of title molecule L using molecular orbital package (MOPAC) software [44,45]. This semi-empirical approach was carried out by creating a Z-matrix of the molecule which was then converted to its MOPAC input data. Optimization of these data had provided the specific bond distance, bond angle and dihedral angle of the most stable molecular geometry. The heat formation energy was generated −145.21 kcals/mole using PM7 method. MOPAC calculations generated visual models of the most stable molecular geometry in ball and stick configuration as shown in Fig. S8 (ESI†).

3.13.1. Molecular docking study

Molecular docking of the free ligand (L) with different receptors has done by Hex 8.0 software. Docking is the process of fitting together of two molecules in 3-dimensional space. It explored ways in which two molecules, such as drugs and protein receptor fit together and docked to each other well. The molecule binding to a receptor, inhibits its function, and thus acts as drug. The collection of different human estrogen protein structures (2Q6J, 2Q98, 2QAB, 2QGT and 4DMA) from the protein data bank and docked with ligand L. It was evaluated using molecular dynamics, by their binding affinities, free energy simulations and relative stabilities. The energy values obtained by docking study was tabulated in Table S5 revealing the best ligand structure fitting was due to 4DMA (−400.05 kcal/mol) compare to other receptors. The molecular docking pose of 2Q6J, 2Q98, 2QAB, 2QGT and 4DMA with molecule L as shown in Fig. S9 (ESI†). The docking results will give potential application of L for protein receptor of human lung cancer cell 4DMA apart from recognition and determination Pr^{3+} and As^{3+}.

4. Conclusion

In summary, we have successfully synthesized and characterized a lower rim functionalized calix [4]arene armed with two naphthoicacid groups which work as fluorogenic units. The probe displays CHEF-PET phenomena. The sensing properties of our fluorescence probe is confirmed by fluorescence titration as well as UV–vis titration and competitive study. Proposed fluorescence probe has lower sensing limit as well as high selectivity towards 1.45 nM for Pr^{3+} and 1.91 nM for As^{3+}. Binding constants with strongly interacting ions were determined by fluorescence titration via PET and CHEF mechanism. The possible molecular structure of the Pr^{3+} and As^{3+} complex is proposed on the basis of ESI-Mass, FT-IR and PXRD. Furthermore, the present system has been applied for

different soil samples for selective determination of Pr^{3+} and As^{3+} with 94–99% recovery. The molecular docking results displayed that the good interaction between title molecule L and protein receptor of human lung cancer cell 4DMA with energy value of −400.05 kcal/mol. This highly sensitive, selective, easy and cost-effective fluorometric method will provide great interest for routine analysis of Pr^{3+} and As^{3+}.

Acknowledgement

P. G. Sutariya would like to acknowledge Department of Science and Technology - Science and Engineering Research Board (DST-SERB) for providing financial assistance under Young Scientist Scheme (YSS/2015/001258) (New Delhi).

Appendix A. Supplementary data

Supplementary data to this article can be found online at https://doi.org/10.1016/j.molstruc.2019.127053.

References

[1] R. Joseph, C.P. Rao, Ion and molecular recognition by lower rim 1,3-Di-conjugates of calix[4]arene as receptors, Chem. Rev. 111 (2011) 4658–4702, https://doi.org/10.1021/cr1004524.
[2] J.P. Chinta, B. Ramanujam, C.P. Rao, Structural aspects of the metal ion complexes of the conjugates of calix[4]arene: crystal structures and computational models, Coord. Chem. Rev. 256 (2012) 2762–2794, https://doi.org/10.1016/j.ccr.2012.09.001.
[3] P.G. Sutariya, A. Pandya, V.A. Rana, S.K. Menon, The Influence of Linking Group in Exterior Point on Mesogenic Properties of the Basket Moulded Molecules: Calix[4]arene, Liquid Crystals, vol. 40, 2013, pp. 374–383, https://doi.org/10.1080/02678292.2012.749305.
[4] P.G. Sutariya, N.R. Modi, A. Pandya, V.A. Rana, S.K. Menon, Synthesis, mesomorphism and dielectric behaviour of novel basket shaped scaffolds constructed on lower rim azocalix[4]arenes, RSC Adv. 3 (2013) 4176, https://doi.org/10.1039/c3ra22422h.
[5] P.G. Sutariya, A. Pandya, A. Lodha, S.K. Menon, A simple and rapid creatinine sensing via DLS selectivity, using calix[4]arene thiol functionalized gold nanoparticles, Talanta 147 (2016) 590–597, https://doi.org/10.1016/j.talanta.2015.10.029.
[6] J.F. Ferreira, I.A. Bagatin, A Cr(VI) selective probe based on a quinoline-amide calix[4]arene, Spectrochim. Acta A Mol. Biomol. Spectrosc. 189 (2018) 44–50, https://doi.org/10.1016/j.saa.2017.07.056.
[7] R. Kumar, M. Arora, A.K. Jain, J.N. Babu, 1,3-Bis(cyanomethoxy)calix[4]arene capped CdSe quantum dots for the fluorogenic sensing of fluorene, RSC Adv. 7 (2017) 14015–14020, https://doi.org/10.1039/C7RA00596B.
[8] A.J. Howarth, T.C. Wang, S.S. Al-Juaid, S.G. Aziz, J.T. Hupp, O.K. Farha, Efficient extraction of sulfate from water using a Zr-metal–organic framework, Dalton Trans. 45 (2016) 93–97, https://doi.org/10.1039/C5DT04163E.
[9] A.N. Alodhayb, M. Braim, L.Y. Beaulieu, G. Valluru, S. Rahman, A.K. Oraby, P.E. Georghiou, Metal ion binding properties of a bimodal triazolyl-functionalized calix[4]arene on a multi-array microcantilever system. Synthesis, fluorescence and DFT computation studies, RSC Adv. 6 (2016) 4387–4396, https://doi.org/10.1039/C5RA12685A.
[10] I.M. Walton, J.M. Cox, C.A. Benson, D. (Dan) G. Patel, Y.-S. Chen, J.B. Benedict, The role of atropisomers on the photo-reactivity and fatigue of diarylethene-based metal–organic frameworks, New J. Chem. 40 (2016) 101–106, https://doi.org/10.1039/C5NJ01718A.
[11] D. Radziuk, H. Möhwald, Ultrasonically treated liquid interfaces for progress in cleaning and separation processes, Phys. Chem. Chem. Phys. 18 (2016) 21–46, https://doi.org/10.1039/C5CP05142H.
[12] K.-C. Chang, L.-Y. Luo, E.W.-G. Diau, W.-S. Chung, Highly selective fluorescent sensing of Cu^{2+} ion by an arylisoxazole modified calix[4]arene, Tetrahedron Lett. 49 (2008) 5013–5016, https://doi.org/10.1016/j.tetlet.2008.06.060.
[13] O. Sahin, M. Yilmaz, Synthesis and fluorescence sensing properties of novel pyrene-armed calix[4]arene derivatives, Tetrahedron 67 (2011) 3501–3508, https://doi.org/10.1016/j.tet.2011.03.035.
[14] R. Miao, Q.-Y. Zheng, C.-F. Chen, Z.-T. Huang, A novel calix[4]arene fluorescent receptor for selective recognition of acetate anion, Tetrahedron Lett. 46 (2005) 2155–2158, https://doi.org/10.1016/j.tetlet.2005.01.138.
[15] J. Fitter, A. Katranidis, T. Rosenkranz, D. Atta, R. Schlesinger, G. Büldt, Single molecule fluorescence spectroscopy: a tool for protein studies approaching cellular environmental conditions, Soft Matter 7 (2011) 1254–1259, https://doi.org/10.1039/C0SM00538J.
[16] D. Atta, A. Okasha, Single molecule laser spectroscopy, Spectrochim. Acta 135 (2015) 1173–1179, https://doi.org/10.1016/j.saa.2014.07.085.
[17] A. Katranidis, D. Atta, R. Schlesinger, K.H. Nierhaus, T. Choli-Papadopoulou, I. Gregor, M. Gerrits, G. Büldt, J. Fitter, Fast biosynthesis of GFP molecules - a single molecule fluorescence study, Angew. Chem. Int. Ed. 48 (2009) 1758–1761, https://doi.org/10.1002/anie.200806070.
[18] D. Atta, F. Gomaa, H. Elhaes, M. Ibrahim, Effect of hydrated dioxin on the physical and geometrical parameters of some amino acids, JCTN 14 (2015) 2405–2408, https://doi.org/10.1166/jctn.2017.6840.
[19] A.B. Othman, J.W. Lee, J.-S. Wu, J.S. Kim, R. Abidi, P. Thuéry, J.M. Strub, A. Van Dorsselaer, J. Vicens, Calix[4]arene-Based, Hg $^{2+}$ -induced intramolecular fluorescence resonance energy transfer chemosensor, J. Org. Chem. 72 (2007) 7634–7640, https://doi.org/10.1021/jo071226o.
[20] S.K. Kim, S.H. Kim, H.J. Kim, S.H. Lee, S.W. Lee, J. Ko, R.A. Bartsch, J.S. Kim, Indium(III)-Induced fluorescent excimer formation and extinction in calix[4]arene–fluoroionophores, Inorg. Chem. 44 (2005) 7866–7875, https://doi.org/10.1021/ic050702v.
[21] J.K. Choi, S.H. Kim, J. Yoon, K.-H. Lee, R.A. Bartsch, J.S. Kim, A PCT-based, pyrene-armed calix[4]crown fluoroionophore, J. Org. Chem. 71 (2006) 8011–8015, https://doi.org/10.1021/jo060981j.
[22] Y. Fu, Z. Xing, C. Zhu, H. Yang, W. He, C. Zhu, Y. Cheng, A novel calixsalen macrocycle: metal sensing behavior for Zn2+ and intracellular imaging application, Tetrahedron Lett. 53 (2012) 804–807, https://doi.org/10.1016/j.tetlet.2011.12.005.
[23] V.K. Gupta, R.N. Goyal, M.K. Pal, R.A. Sharma, Comparative studies of praseodymium(III) selective sensors based on newly synthesized Schiff's bases, Anal. Chim. Acta 653 (2009) 161–166, https://doi.org/10.1016/j.aca.2009.09.008.
[24] M.R. Ganjali, P. Norouzi, F.S. Mirnaghi, S. Riahi, F. Faridbod, Lanthanide recognition: monitoring of praseodymium(III) by a novel praseodymium(III) microsensor based on N$'$-(Pyridin-2-Ylmethylene)Benzohydrazide, IEEE Sens. J. 7 (2007) 1138–1144, https://doi.org/10.1109/JSEN.2007.897950.
[25] E. Majid, S. Hrapovic, Y. Liu, K.B. Male, J.H.T. Luong, Electrochemical determination of arsenite using a gold nanoparticle modified glassy carbon electrode and flow analysis, Anal. Chem. 78 (2006) 762–769, https://doi.org/10.1021/ac0513562.
[26] B. Mandal, Arsenic round the world: a review, Talanta 58 (2002) 201–235, https://doi.org/10.1016/S0039-9140(02)00268-0.
[27] C.D. Kozul, T.H. Hampton, J.C. Davey, J.A. Gosse, A.P. Nomikos, P.L. Eisenhauer, D.J. Weiss, J.E. Thorpe, M.A. Ihnat, J.W. Hamilton, Chronic exposure to arsenic in the drinking water alters the expression of immune response genes in mouse lung, Environ. Health Perspect. 117 (2009) 1108–1115, https://doi.org/10.1289/ehp.0800199.
[28] P.G. Sutariya, A. Pandya, N.R. Modi, S.K. Menon, A highly efficient PET switch on–off–on fluorescence receptor based on calix[4]arene for the selective recognition of Cd^{2+} and Sr^{2+}, Analyst 138 (2013) 2244, https://doi.org/10.1039/c3an00091e.
[29] P.G. Sutariya, A. Pandya, A. Lodha, S.K. Menon, A pyrenyl linked calix[4]arene fluorescence probe for recognition of ferric and phosphate ions, RSC Adv. 4 (2014) 34922–34926, https://doi.org/10.1039/C4RA04546G.
[30] P.G. Sutariya, A. Pandya, A. Lodha, S.K. Menon, A unique fluorescence biosensor for selective detection of tryptophan and histidine, Analyst 139 (2014) 4794–4798, https://doi.org/10.1039/C4AN00829D.
[31] P.G. Sutariya, N.R. Modi, A. Pandya, B.K. Joshi, K.V. Joshi, S.K. Menon, An ICT based "turn on/off" quinoline armed calix[4]arene fluoroionophore: its sensing efficiency towards fluoride from waste water and Zn^{2+} from blood serum, Analyst 137 (2012) 5491, https://doi.org/10.1039/c2an36247c.
[32] P.G. Sutariya, A. Pandya, A. Lodha, S.K. Menon, Fluorescence switch on–off–on receptor constructed of quinoline allied calix[4]arene for selective recognition of Cu^{2+} from blood serum and F– from industrial waste water, Analyst 138 (2013) 2531, https://doi.org/10.1039/c3an00209h.
[33] P.G. Sutariya, H. Soni, S.A. Gandhi, A. Pandya, Novel luminescent paper based calix[4]arene chelation enhanced fluorescence- photoinduced electron transfer probe for Mn^{2+}, Cr^{3+} and F-, J. Lumin. 208 (2019) 6–17, https://doi.org/10.1016/j.jlumin.2018.12.009.
[34] P.G. Sutariya, H. Soni, S.A. Gandhi, A. Pandya, Single-step fluorescence recognition of as $^{3+}$, Nd $^{3+}$ and Br $^{-}$ using pyrene-linked calix[4]arene: application to real samples, computational modelling and paper-based device, New J. Chem. 43 (2019) 737–747, https://doi.org/10.1039/C8NJ03506G.
[35] S.M. Darjee, K.M. Modi, U. Panchal, C. Patel, V.K. Jain, Highly selective and sensitive fluorescent sensor: thiacalix[4]arene-1-naphthalene carboxylate for Zn 2+ ions, J. Mol. Struct. 1133 (2017) 1–8, https://doi.org/10.1016/j.molstruc.2016.11.028.
[36] P. Thordarson, Determining association constants from titration experiments in supramolecular chemistry, Chem. Soc. Rev. 40 (2011) 1305–1323, https://doi.org/10.1039/C0CS00062K.
[37] P.G. Sutariya, H. Soni, S.A. Gandhi, A. Pandya, Novel tritopic calix[4]arene CHEF-PET fluorescence paper based probe for La^{3+}, Cu^{2+}, and Br^{-}: its computational investigation and application to real samples, J. Lumin. 212 (2019) 171–179.
[38] D. Maity, A. Chakraborty, R. Gunupuru, P. Paul, Calix[4]arene based molecular sensors with pyrene as fluoregenic unit: effect of solvent in ion selectivity and colorimetric detection of fluoride, Inorg. Chim. Acta 372 (2011) 126–135, https://doi.org/10.1016/j.ica.2011.01.053.
[39] H. Ali Zamani, M. Masrournia, S. Sahebnasagh, M. Reza Ganjali, Fabrication of a praseodymium(III) PVC-membrane sensor based on N′ 1 ,N′ 2 -Bis(2-oxo-1,2-diphenylethylidene) ethanedihydrazide, Anal. Lett. 42 (2009) 555–570, https://doi.org/10.1080/00032710802677092.

[40] V.K. Gupta, R.N. Goyal, M.K. Pal, R.A. Sharma, Comparative studies of praseodymium(III) selective sensors based on newly synthesized Schiff's bases, Anal. Chim. Acta 653 (2009) 161–166.
[41] K. Chauhan, P. Singh, B. Kumari, R.K. Singhal, Synthesis of new benzothiazole Schiff base as selective and sensitive colorimetric sensor for arsenic on-site detection at ppb level, Anal. Methods 9 (2017) 1779–1785, https://doi.org/10.1039/C6AY03302D.
[42] D.X.O. Jaramillo, A. Sukeri, L.P.H. Saravia, P.J. Espinoza-Montero, M. Bertotti, Nanoporous gold microelectrode: a novel sensing platform for highly sensitive and selective determination of arsenic (III) using anodic stripping voltammetry, Electroanalysis 29 (2017) 2316–2322, https://doi.org/10.1002/elan.201700301.
[43] T.A. Ivandini, R. Sato, Y. Makide, A. Fujishima, Y. Einaga, Electrochemical detection of arsenic(III) using iridium-implanted boron-doped diamond electrodes, Anal. Chem. 78 (2006) 6291–6298.
[44] D.A. Kotadia, U.H. Patel, S. Gandhi, S.S. Soni, Pd doped SiO 2 nanoparticles: an efficient recyclable catalyst for Suzuki, Heck and Sonogashira reactions, RSC Adv. 4 (2014) 32826–32833.
[45] U.H. Patel, S.A. Gandhi, V.M. Barot, M.C. Patel, A comparative study of novel chalcone derivative by X-ray and quantum chemical calculations (Ab-initio and DFT): experimental and theoretical approach, Mol. Cryst. Liq. Cryst. 624 (2016) 190–204.